APPLICATION OF PULSED FLASH THERMOGRAPHY METHOD FOR SPECIFIC DEFECT ESTIMATION IN ALUMINUM

by

Ljubiša D. TOMIĆ[a*], Dalibor B. JOVANOVIĆ[a], Radovan M. KARKALIĆ[b], Vesna M. DAMNJANOVIĆ[c], Branko V. KOVAČEVIĆ[d], Dalibor D. FILIPOVIĆ[e], and Sonja S. RADAKOVIĆ[f]

[a] Technical Testing Centre, Belgrade, Serbia
[b] Military Academy, University of Defense, Belgrade, Serbia
[c] Faculty of Mining and Geology, University of Belgrade, Belgrade, Serbia
[d] CBRN Defense Centre, Krusevac, Serbia
[e] Serbian Armed Forces, Nis, Serbia
[f] Medical Faculty of the Military Medical Academy, University of Defense, Belgrade, Serbia

Original scientific paper
DOI: 10.2298/TSCI150307080T

Non-destructive thermal examination can uncover the presence of defects via temperature distribution profile anomalies that are created on the surface as a result of a defect. There are many factors that affect the temperature distribution map of the surface being tested by infrared thermography. Internal defect properties such as thermal conductivity, heat capacity, and defect depth play an important role in the temperature behavior of the pixels or regions being analyzed. Also, it is well known that other external factors such as the convection heat transfer, variations on the surface emissivity, and ambient radiation reflectivity can affect the thermographic signal received by the infrared camera. In this paper, we considered a simple structure in the form of flat plate covered with several defects, whose surface we heated with a uniform heat flux impulse. We conducted a theoretical analysis and experimental test of the method for case of defects on an aluminum surface. First, experiments were conducted on surfaces with intentionally created defects in order to determine conditions and boundaries for application of the method. Experimental testing of the pulsed flash thermography method was performed on simulated defects on an aluminum test plate filled with air and organic compound n-hexadecane, hydrocarbon that belongs to the phase change materials. Study results indicate that it is possible, using the pulsed flash thermography method, to detect the type of material inside defect holes, whose presence disturbs the homogeneous structure of aluminum.

Key words: *infrared thermography, non-destructive testing, defect estimation, pulsed flash thermography, phase change material*

Introduction

Impulse method of measuring thermal diffusion attracted a great interest when it was first introduced in a research in 1961 [1]. First non-contact measurement with impulse radiometry was performed in 1962 when it was also published for the first time [2]. In the works that followed a new technique of impulse radiometry where the source and IC detector were on the same side of the sample, was mentioned for the first time, and soon after a theoretical

* Corresponding author; e-mail: ljubisa.tomic@gmail.com

model for infrared (IR) signal analysis was developed [1-3]. With the introduction of TV compatible thermal imaging sensors with *signal processing in the element* detectors, new possibilities for application of thermal impulse technique were opened which brought up new developments of the technique in numerous studies [4-6].

Infrared thermography (IRT) is one of more advanced methods of non-destructive testing (NDT). The IRT applies to NDT measure and interprets the temperature field of the surface of the body being tested. The NDT based on IRT can be applied using either a passive or an active approach. The passive approach is used, for example, in the inspection of aircraft structures to discover presence of water inside panels. Byte typical active approach, the IR radiation locally emitted from the surface of a sample which has been stimulated by a thermal perturbation is detected by means of an IR camera which provides images, known as thermograms. In active approach (active thermography), acquisition is carried out at the same time as an external stimulus is being applied to the inspected specimen. The objective is to create a thermal contrast on subsurface anomalies, *i. e.*, the defects. Many different stimulation methods can be applied and most of them can be classified as optical, mechanical, or inductive. The most common methods are based on optical stimulation, which uses light to deliver energy to the specimen [7].

The IRT is a technique, which has the advantage of good defect detection possibility along with the capacity to inspect a large area within a short time. To inspect defects over a large-scale and at large stand-off distances, integration of Iran other NDT approaches have been investigated [8-10], for example, pulsed flash thermography [11-15, 16-21], vibrothermography, sonic thermography, laser thermography, and pulsed-eddy-current (PEC) stimulated thermography [22].

Pulsed thermography is an NDT method, which involves briefly heating the specimen with a short pulse of thermal stimulation and then recording the temperature decay curve [8, 9, 16-22]. The temperature in the material varies rapidly after the initial thermal pulse, while the thermal front propagates by diffusion through the material. The presence of a discontinuity will change its local diffusion rate, so that, by observing the temperature of the surface, the discontinuities appear to be among the areas of different temperatures with respect to its surrounding areas.

Nowadays this method is usually called pulsed flash thermography (PFT). In this paper we described basic principles and gave some examples of PFT application on materials with wide spectra of thermal properties. The objective of the study is to determine the influence of *n*-hexadecane on the surface temperature distribution and the value of the maximum temperature difference. Hydrocarbon *n*-hexadecane is a material from the phase change materials (PCM), which are regarded as a possible solution for reducing the energy consumption of buildings. The presence of *n*-hexadecane inside defect hole changes the shape of the temperature contrast in time, with respect to the temperature contrast when the hole is empty (*i. e.* filled with air). We assumed that it is possible, using the PFT method, to detect the type of material in the defect holes, whose presence disturbs the homogeneous structure of aluminum.

Pulsed flash thermography

Key property that distinguishes PFT from other methods is direct measurement. Shape of the time-dependent surface temperature curve depends on the extent of penetration of excitement radiation into the examined material, thermal diffusivity and transmission for emitted IR radiation of the material. Time-dependent surface temperature is a source of information about material defects.

General scheme of the measurements is shown in fig. 1.

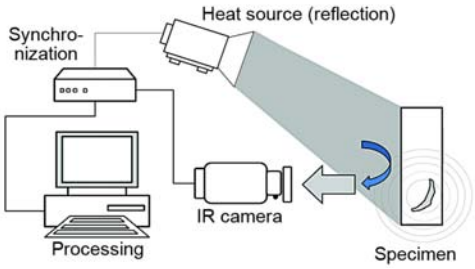

Figure 1. General structure of the system for analysis of defects through application of PFT method

Heat transfer in the presence of defects

Heat conduction in solid bodies without heat source is described as the Fourier's law equation [13, 14]:

$$\frac{\partial\theta}{\partial t}=\frac{k}{c\rho}\left(\frac{\partial^2\theta}{\partial x^2}+\frac{\partial^2\theta}{\partial y^2}+\frac{\partial^2\theta}{\partial z^2}\right) \tag{1}$$

where θ, k, c, and ρ are the temperature rise, heat conductivity, specific heat, and volumetric mass density, respectively, and term $c\rho$ is the volumetric temperature capacity.

If we assume that heat flow in y- and z-direction is negligible (in reality this would means that dimensions of the flashed surface have to be large in comparison to the depth of the penetration of the examined radiations) and that the contributions to the heat flow from thermal radiation and from contact at $x = 0$ with air or other materials are negligible, we can use an equation for 1-D heat conduction. Initial temperature distribution right after the excitation, disregarding non-linear effect such as transition (short lasting) phases, is:

$$\theta(x)=\theta_0\ \exp(-ax) \tag{2}$$

where $\theta_0 = E_0\, a/c\rho$ is the initial surface temperature increase, E_0 – the input energy per unit area, and a – the thermal diffusivity.

To prepare material for testing with PFT, you need to know two variables: one is amount of heat that need transfer to the unit of surface to get wanted level of contrast, and the other is the last time necessary to develop that contrast on the sample surface. Time $t_{1/2}$, which it takes for the temperature of the opposite surface to reach half of its maximum, for a plate of L thickness, is calculated by the equation [1-3, 12]:

$$t_{1/2}=\frac{1.38L^2}{\pi^2 a} \tag{3}$$

Because impulse light sources transfer energy to heat in very short time intervals, to avoid too big increase in initial temperature having destructive effects on the materials, there should be pre calculated maximum temperatures of the front side (θ_f) for impulses of different shape.

For triangularly shaped impulse we get [3-10]:

$$\theta_f=\frac{8Q}{3\beta c\rho(2\pi a y)^{1/2}} \tag{4}$$

where Q is the energy transferred per unit of surface, y – the effective flash time, and β – an impulse profile parameter.

Materials for defects analysis

For examination of defect with PFT method we can use different materials with broad spectrum [15]. Especially important are materials which are being used for the purpose

of thermoregulation because they require special thermophysical properties. The PCM possess the ability to change their state within a certain temperature range. These materials absorb energy during the heating process as phase change takes place, otherwise this energy can be transferred to the environment in the phase change range during a reverse cooling process [23]. The large heat transfer during the melting process as well as the crystallization process without significant temperature changes makes PCM interesting as a source of heat storage material in practical applications [24]. A wide spectrum of PCM is available with different heat storage capacities and phase change temperatures.

For the needs of our study investigation, we used an organic PCM based on *n*-hexadecane, mixture that belongs to the paraffin hydrocarbons. Paraffin's are regarded as a possible solution for reducing the energy consumption of buildings. By storing and releasing heat within a certain temperature range, it raises the building inertia and stabilizes indoor climate.

Efficient use of PCM paraffin microcapsules is to encase and insert them into the ceiling. Because paraffin is flammable, a PCM insert must be placed in between two plates of good fire retardant material, such as metal. Metal plate also offers good heat conductivity so it draws heat inside, to the PCM material [25].

Table 1 shows values of thermal conductivity, density and specific heat of alumina, air, *n*-hexadecane and some other materials which are suitable for examination with PFT method.

Table 1. Thermophysical properties of materials that can be used with PFT

Material	Specific heat c [$Jkg^{-1}°C^{-1}$]	Density ρ [kgm^{-3}]	Volumetric heat capacity $c\rho$ [$J°C^{-1}m^{3}$]	Thermal conductivity k [$Wm^{-1}°C^{-1}$]	Thermal diffusivity a [m^2s^{-1}]
Soft iron	$0.44\cdot10^3$	$7.9\cdot10^3$	$3.476\cdot10^6$	46	$13\cdot10^{-6}$
Stainless steel	$0.5\cdot10^3$	$7.99\cdot10^3$	$3.995\cdot10^6$	16.2	$4.055\cdot10^{-6}$
Aluminum	$0.88\cdot10^3$	$2.7\cdot10^3$	$2.376\cdot10^6$	230	$95\cdot10^{-6}$
Water	$4.17\cdot10^3$	$1.0\cdot10^3$	$4.17\cdot10^6$	0.6-0.68	$0.144\cdot10^{-6}$
Air	$1.005\cdot10^3$	$0.01125\cdot10^3$	$0.011\cdot10^6$	0.0257	$2.273\cdot10^{-6}$
n-hexadecane	$2.31\cdot10^3$	$0.77344\cdot10^3$	$1.786\cdot10^6$	0.15	$0.084\cdot10^{-6}$

Table 2. Thermal raise times and surface temperatures for PFT usable materials

Material	$t_{1/2}$ [s] (i)	θ_f [°K] (ii)	Th [mm] (iii)
Soft iron	1.1	9.6	0.30
Stainless steel	2	13.0	0.22
Aluminum	0.15	5.2	0.80
Water	97.2	77.4	0.03
Air (C_v)	6.16	26.46	0.47
n-hexadecane	166.62	235.8	0.0237

Considering that flash time is so short that only shallow surface layer will be exposed to high temperature. Table 2 gives values for time $t_{1/2}$ (time needed to raise temperature of opposite surface to half of the maximum value, for a plate of L thickness) [2, 10].

Values shown in tab. 2 for different materials are annotated: (i) $t_{1/2}$, in seconds for thin plates 1 cm in thickness, (ii) θ_f, maximal temperature of the front side θ_f with 6 ms of flash deposition (depositing 1 J/cm^2), and (iii) Th, thickness of material heated to temperature θ_f.

Temperature difference ΔT is defined as the difference in temperature between the area on the surface over the defect and over the sound material. Analysis of the time depend-

ence of the temperature difference change $\Delta T(t)$, gives us the possibility of determining the depth of the defect. The temperature difference is changing over time, reaching a maximum value ΔT_{max}. The maximum temperature difference, ΔT_{max} is the specific parameter which depends on the defect depth and the type of materials by which defects holes are filled. The temperature difference, $\Delta T(t)$ is an important parameter for the defect quantitative analysis, whose extreme values (minimum or maximum) represent the time t at which the reflection of the defect on the material surface is most clearly seen.

Experimental equipment

Experimental equipment contains heat source (two BOWENS BW-3955 Gemini R & Pro Flashes), IR camera which detects emitted IR radiation of the test plate (TP) heated surface and accompanies the surface cooling process, as well as a computer registering digital data in real time.

We used a camera "FLIR SC620" intended to work in wavelengths 7.5-13 μm, which contains uncooled microbolometar detector, known as focal matrix in focal plane (640×480 semiconductor detectors) and standard optics 24°×18°. Measurement results can be shown on a camera screen as a thermogram or coded scales (in shades of gray or in color), which can be converted in temperature values with the use of appropriate tables [13, 16, 17]. Positioning two photographic flashes approximately 20 cm apart under 45° angle with regard to heated surface gives an ability to homogenously heat the surface. Computer controlled synchronization allows for simultaneous triggering of two impulse light sources-flashes. It is possible to move the flashes vertically as well.

According to technical properties max power of the flash is 1500 W. Time differential between two consecutive light pulses is 2.8 ms, since frequency of light pulse is 357.142 Hz. Considering that duration of one frame t_f of thermal visioning camera is significantly longer (three modes of operation, 8.33 ms, 16.66 ms, and 33.33 ms), we conclude that a condition that impulse duration must be much shorter than t_f was met. Measurements were taken in two modes of operation: 8.33 ms and 16.66 ms. Duration of light impulse at max power is 1/1400 (0.7142 ms). For the sake of focus of light flux on the TP, we mounted a reflector with a 20 cm opening on the flash source.

Thermal imaging camera does conversion of spatial non-homogeneous distribution of flux of its own radiation of the scene into a visible picture. Significant parameters for collecting base of thermogram (recording) are temperature of the heated TP surface, reflexivity of the TP, emissivity, ambient temperature, relative humidity, and distance of the TP from the camera. Measurements shown in this study were conducted on short distances (approximately 50 cm), so distance as a parameter does not have a major influence. Temperature and emissivity of TP were estimated by thermal visioning camera. Max thermogram transfer frequency from the camera to the computer during the recording was 60 Hz while memory was 12 bits for every pixel. Experimental set-up with flash pulsed thermography system established for the testing purposes is shown in fig. 2. Such system allows testing the influence of *n*-hexadecane in aluminum plate on the temperature contrast. The IR camera was set-up in front of the aluminum plate so that you could track IR imaging of the field of vision on computer display (TP thermogram).

In order to get optimal TP picture sharpness we manually zoomed and set-up recording parameters: ambient temperature, emissivity, distance, and air humidity. Recording is initiated by remote radio trigger Pulsar Radio Trigger System, which operates on 433 MHz and is used for synchronized triggering of two BW 3967 flashes. Recording was done in a labora-

tory with a 25.9 °C temperature, 50% humidity which allowed sub cooled *n*-hexadecane to be in solid state in the cooler which enabled experiment to run smoothly.

Testing piece

The TP is made out of aluminum, size 180 mm × 50 mm × 8.3 mm. Simulated defects are hollow cylindrical spaces (circular holes series: A, B, C, D, and E) with flat bottom (fig. 3).

Figure 2. Flash pulsed thermography system

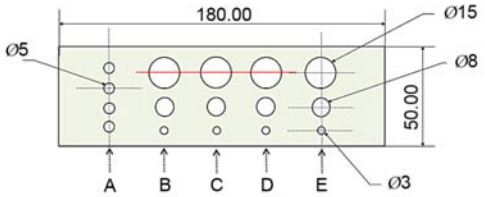

Figure 3. Scheme of the aluminum TP

Holes have different diameters, but holes of the same series have identical depths. Series A has four holes with identical diameter of 5 mm, while series B, C, D, and E all have three holes with differing diameters of 15 mm, 8 mm, and 3 mm. Series of measurements was made on a shown TP. Horizontal line in fig. 3 is a line that marks the place where the readings of thermogram temperatures are made. In order to decrease reflection, surfaces of aluminum TP were painted black. After eloxing with KERN vernier with accuracy 0.01 mm and micrometer IP40 ORION® with accuracy 0.001 mm, we measured defect dimensions (tab. 3).

Table 3. Dimensions of simulated defects in aluminum plate with 8.3 mm thickness

Defects A		Defects B×	Defects C	Defects D	Defects E
D = ∅5	*d* = 1.5 mm	*d* = 0.5 mm	*d* = 0.8 mm	*d* = 1.1 mm	*d* = 1.5 mm
	d = 1.1 mm	*D* = ∅3	*D* = ∅3	*D* = ∅3	*D* = ∅3
	d = 0.8 mm	*D* = ∅8	*D* = ∅8	*D* = ∅8	*D* = ∅8
	d = 0.5 mm	*D* = ∅15	*D* = ∅15	*D* = ∅15	*D* = ∅15

In tab. 3, *D* represents hole diameter, while *d* is depth of the cylindrical hole (defect) in aluminum. First we analyzed a plate with empty defects, *i. e.* they had ambient temperature air in them. After that we filled holes of *D* = ∅15 and ∅8 mm diameters from series B, C, D, and E with 50% *n*-hexadecane, and after that with 100% *n*-hexadecane. By method of impulse thermography using IR camera we recorded temperature change on aluminum plate surface right above the defects, in areas with no defects and above defects filled with 50% and 100% *n*-hexadecane. We measured emissivity of the aluminum plate surface of 0.97 by using thermographic method with a tape over a surface of known emissivity.

Results

We performed selection and analysis of IR recordings by using software for analysis of recorded sequences ThermaCam 2.10 on a personal computer. Results of the experiment can be saved on a memory flash drive and PC hard drive so that you can analyze it in real time later on. Selected scenes were isolated by IR picture manipulation software. We applied method of pulse thermography on an aluminum plate previously cooled to 15.9 °C, which was 9.7 °C colder than ambient temperature which was 25.6 °C.

Figure 4 shows 52nd frame of the recorded sequence before the lighting with the BW-3955 flash. It was triggered by radio trigger-pulsar for remote triggering in order to eliminate any effect on light that operator could have.

The plate was previously cooled to 15.9 ºC, 52nd frame seq.011 is one frame before the flash was triggered. The figure shows the surface before it was radiated with light impulse, it can be noticed that the pixel temperature of that surface is approximately even at the noise level as well.

The 56th frame of the recorded sequence seq. 011, four frames after the trigger of the flash, is shown in fig. 5. The plate was previously cooled to 15.9 ºC. On the left side going from bottom to top you can notice blurred reflections of the defects with diameter D = ∅5. Figures 4 and 5 show circular marked areas AR01, AR02, AR03, and AR04 from left to right in the middle of the temperature reflection from lowest to highest defect depth. All with the same hole diameter D = ∅15 mm, these represent a defect area of an average temperature from 18.2 °C to 17.1 °C. Marked circle AR05, above defect less area shows average temperature in that part of aluminum plate, which is 16.9 °C.

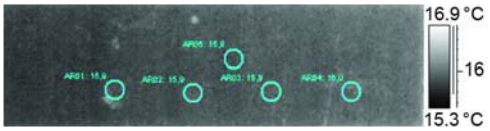

Figure 4. Thermogram of the 52nd frame of the recorded seq.011 before the lighting with BW-3955 flash sources

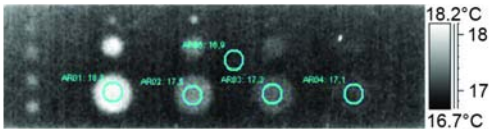

Figure 5. Thermogram of the 56th frame of recorded seq.011 after the lighting with BW-3955 flash sources, lighted by radio remote trigger

Figure 5 also shows thermogram of the 56th frame chosen from a series of measurements in recorded sequence seq.0011 (from the total of 488 frames in the sequence). Total sequence duration time before and after the heating with light impulse is 4066.66 ms. Thermogram presented in fig. 5 was recorded 33.33 ms from the start of the heating. Shallow defects that can be seen on thermogram shortly after cooling by internal diffusion have visible shapes.

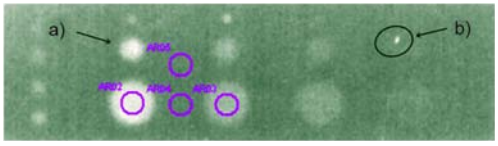

Figure 6. Thermal image of aluminum test sample, fourth frame after a light pulse

Figure 6 shows a thermogram of the 56th frame (fourth frame after the lighting of aluminum test sample with light impulse), like in fig. 5 in recorded sequence seq.0011.

On the picture of the aluminum test sample after the lighting of the surface with light impulse defect contours are easily spotted as places warmer than surfaces without defects. Defect with 8 mm diameter is marked with (a) on the thermogram, while place on the thermogram marked with (b) shows an irregularly shaped hot spot as a fake noise caused by non-homogeneous emissivity of the surface.

Figure 7 shows graphs of temperature differences as a function of time for average pixel temperatures in areas AR02 and AR05 for holes 15 mm in diameter, as well as the temperature difference of areas above the 8 mm hole and areas away from defects (AR05). Max temperature difference, represents a parameter of quantitative determination of defect width. For unknown defects first you need to determine dependence of max temperature changes of known diameters so that you can use those calibration curves to determine width of unknown defects. For holes of 15 mm wide, ΔT_{max} = 1.34 °C, while for holes of 8 mm wide,

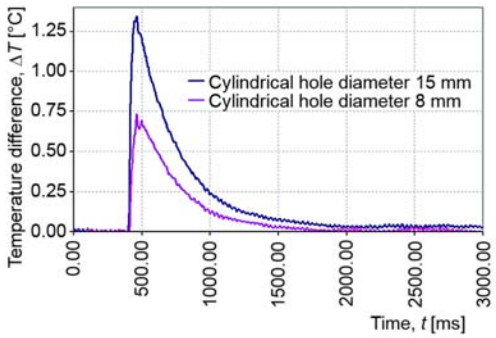

Figure 7. Temperature difference as a function of time between a defect and a no-defect area for cylindrical defects with 15 and 8 mm holes *(for color image see journal web-site)*

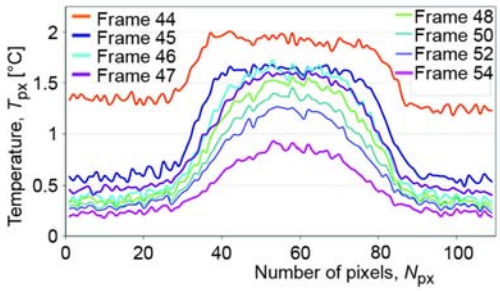

Figure 8. Temperature profile along the line of pixels that runs through the center of the defect shape circle between defect and no-defect area *(for color image see journal web-site)*

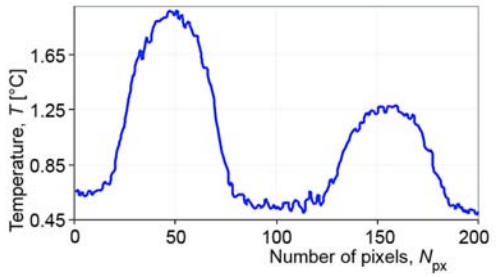

Figure 9. Temperature profile along the central line of the two widest defects at depths *d* = 0.5 mm and 0.8 mm

ΔT_{max} = 0.73 °C, their ration is approximately proportional to the ratio of defect diameters. The upper curve represents temperature difference between area above defect AR02 of the heated surface and no-defect area as a function of time, as shown in fig. 6.

Accurate determination of max temperature difference is not possible within a single frame, because commercial IR camera lacks external trigger and consequently, the possibility of synchronization of start frame and a moment of pulse lamp trigger (maximal value of ΔT_{max} is from 458.33 ms to 466.57 ms from the start of sequence seq.0011 recording).

The temperature profile along the line of pixels running through the center of the defect shape circle on thermogram between defect and no-defect area, for cylindrical holes 15 mm in diameter for first eight frames from the moment of light source triggering, is given in fig. 8.

Temperature difference between area above defects and no-defect area is increasing until it reaches maximum value ΔT_{max}, after which it drops off. Slope of the curve depends on the type of defect in material. In our study we treated two types of defects in aluminum plate, air defect and defects with material from PCM group, *n*-hexadecane. For defect depth quantification for defects ∅15 mm in diameter (where ∅ is the cylindrical hole diameter), we considered various depths. The experimental results were compared with [18, 19] simulated results.

Temperature contrast was computed by taking the temperature difference between defective and non-defective areas and plotted as a function of time (fig. 9). For holes 15 mm wide ΔT_{max} = 1.97 °C at depth d = 0.5 mm, while for holes of same width but at depth of d = 0.8 mm, ΔT_{max} = 1.27 °C which is a 37.5% decrease from the max temperature contrast of shallower defects. For defects that are percentage wise deeper, max value of temperature contrast decreases, so that when temperature difference falls below sum level defects will not be visible.

Figure 10 shows graphs of temperature differences as a function of time for average pixel temperatures in areas AR02 and AR05 for holes 15 mm in diameter, when the hole is empty (air), 50% and 100% filled with *n*-hexadecane. Graphs of differences in average tem-

peratures of AR02 area above defect and away from defect, AR04, from fig. 6 as a function of time for recorded sequences seq.0004, seq.0006 and seq.0011 (50% and 100% filled with *n*-hexadecane substance and empty holes).

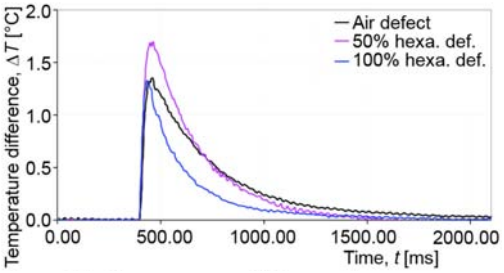

Figure 10. Temperature difference between empty defect and defect with n-hexadecane charge
(for color image see journal web-site)

Conclusions

Thermographic methods like other NDT methods have application difficulties which were summed up [2]. However, PFT method is very applicable considering that it does not require physical contact with the examined material except for the heat transfer, it can also be very quick and can be applied when only one side of the object is accessible. Because of these characteristics the method has become a subject of numerous scientific studies conducted by many researchers, especially in the area of non-destructive testing of multilayer materials which is proven by many studies that applied it successfully [18-21]. But defects with diameter/depth ratios around or less than one are difficult to discover using thermal methods in isotropic materials [2].

This work clearly reveals the potential of pulsed flash thermography for defect estimation in aluminum. In the course of experiments we successfully proved a use of commercial video compatible IR camera in combination with modern high flash intensity light sources for creation of pictures of defects in a second or a portion of a second, with useful solutions for some problems mentioned earlier. We analyzed an experimental set-up in which a main heat source and IR camera are on the same side of the sample. We used a simplified theoretical model for heat transfer in the examined sample which to determine time dependence of sample surface temperature in the presence of defects and with no defects. We constructed experimental samples with simulated defects (plate with hollow spaces of differing diameter and depth).

Experimental results showed that PFT method is applicable for non-destructive discovery of material subsurface defects, but that there are difficulties in application, which are primarily tied to heat and reflection properties of the material as well as to limitations of time resolution of IR camera. In this study, some barriers in the application of PFT method, such as controlling the uniformity of the heating cycle in space and time as well as emissivity variations of the sample surface, were successfully eliminated by optimizing the experiment. Upon completion of experimental research on these samples we planned on conducting a number of experiments with defects on other materials in order to optimize parameters of radiation source and conditions of registering thermal vision pictures. The final goal is to establish conditions for experimental set-up applicable for detection of appropriate classes of defects in different materials.

Nomenclature

a – thermal diffusivity, [m^2s^{-1}]
c – specific heat, [$Jkg^{-1}°C^{-1}$]
$c\rho$ – volumetric heat capacity, [$J°C^{-1}m^{-3}$]
D – defect hole diameter, [mm]
d – defect hole depth, [mm]
k – thermal conductivity, [$Wm^{-1}°C^{-1}$]
ΔT – temperature difference, [°C]
ΔT_{max} – max. temperature difference, [°C]
t – time, [s]

Greek symbols

ρ – density, [kgm^{-3}]
θ_0 – initial temperature rise ($=E_0\,a/c\rho$), [°C]
θ_f – front side max. temperature, [°C]

References

[1] Parker, W. J., *et. al.*, Flash Method of Determining Thermal Diffusivity, Heat Capacity and Thermal Conductivity, *J. Appl. Phys., 32* (1961), 9, pp. 1679-1684
[2] Maldague, X. P., *Theory and Practice of Infrared Technology for Non-Destructive Testing*, John Wiley & Sons, Inc., New York, USA, 2001
[3] Maldague, X., *et. al.*, Subsurface Flaw Detection in Reflective Materials by Thermal Transfer Imaging, *Optical Engineering, 30* (1991), 1, pp. 117-129
[4] Williams, J. H., *et. al.*, One-Dimensional Analysis of Thermal Non-Destructive Detection of Delamination and Inclusion Flaws, *British Journal of NDT, 22* (1980), 3, pp. 113-118
[5] Imhof, R. E., *et. al.*, Optothermal Transient Emission Radiometry, *J. Phys. E: Sci. Instrum., 17* (1984), 6, pp. 521-525
[6] Cielo, P., Pulsed Photothermal Evaluation of Layered Materials, *J. Appl. Phys., 56* (1984), 1, pp. 230-234
[7] Leung, W. P., Tam, A. C., Techniques of Flash Radiometry, *J. Appl. Phys., 56* (1984), 1, pp. 153-161
[8] Meola, C., Carlomagno, G. M., *Recent Advances in Non-Destructive Inspection*, Nova Science Publisher Inc., New York, NY, USA, 2010
[9] Martin, R. E., *et al*., Interpreting the Results of Pulsed Thermography Data, *Materials Evaluation, 61* (2003), 5, pp. 611-616
[10] Burch, S. F., *et. al.*, Detection of Defects by Transient Thermography: A Comparison of Predictions from Two Computer Codes with Experimental Results, *26*, (1984), 1, pp. 36-39
[11] Cielo, P., *et. al.*, Thermographic Non-Destructive Evaluation of Industrial Materials and Structures, *Materials Evaluation, 45* (1987), 4, pp. 452-465
[12] Milne, J. M., Reynolds, W. N., Application of Thermal Pulses and Infrared Thermal Imagers for Observing Sub-Surface Structures in Metals and Composites, *SPIE., 590* (1986), May, pp. 283-327
[13] Carslaw, H. S., Jaeger, J. C., *Conduction of Heat in Solids*, Oxford University Press, Oxford, UK, 1955
[14] Tomić, D. Lj., Non-Destructive Evaluation of the Thermophysics Properties Materials by IR Thermography, Ph. D. thesis, School of Electrical Engineering, University of Belgrade, Belgrade, 2013
[15] Zeng, Z., *et. al.*, Depth Prediction of Non-Air Interface Defect Using Pulsed Thermography, *NDT&E International, 48*, (2012), Jun., pp. 39-45
[16] Minkina, W., Dudzik, S., Simulation Analysis of Uncertainty of Infrared Camera Measurement and Processing Path, *Measurement, 39* (2006), 8, pp. 758-763
[17] Tomić, Lj., *et al*., The Influence of Subsurface Defects in Material on Differences in Numerical and Experimental Detection Results, Applying Pulse Thermography, *Proceedings*, 3rd Conference MediNano, Belgrade, Serbia, 2010, p. 77
[18] Tomić, Lj., Milinović, M., Experimental Research of Limits for Thermal Modulation Transfer Function, *Thermal Science,13* (2009), 4, pp. 119-128
[19] Tomić, Lj., *et al*., Numerical Simulation of the Temperature Field in Pulse Radiometric Defectoscopy, *Proceedings*, 14th International Conference on Aerospace Sciences & Aviation Technology, Cairo, Egypt, 2011, p. 99
[20] Grys, S., New Thermal Contrast Definition for Defect Characterization by Active Thermography, *Measurement, 45* (2012), 7, pp. 1885-1892
[21] Minkina, W., Dudzik, S., *Infrared Thermography: Errors and Uncertainties*, John Wiley & Sons Ltd., London, 2009
[22] Usamentiaga, R., *et. al.*, Infrared Thermography for Temperature Measurement and Non-Destructive Testing, *Sensors, 14* (2014), 7, pp. 12305-12348
[23] Mondal, S., Phase Change Materials for Smart Textiles – An Overview, *Applied Thermal Engineering, 28* (2008), 11-12, pp. 1536-1550
[24] Jovanović, D., *et. al*., Efficacy of a Novel Phase Change Material for Microclimate Body Cooling, *Thermal Science, 18* (2014), 2, pp. 697-705
[25] Zalba, B., *et. al*., Free-Cooling of Buildings with Phase Changing Materials, *International Journal of Refrigeration, 27* (2004), 8, pp. 839-849

Paper submitted: March 7, 2015
Paper revised: May 12, 2015
Paper accepted: May 12, 2015